Coupling of a Macroscopic Solidification Simulation with a Micro Model and Thermodynamic Calculations of Phase Diagrams

Klaus Greven, Andreas Ludwig, Thorsten Hofmeister, Peter R. Sahm
Giesserei-Institut, RWTH Aachen

1. Introduction

Nowadays, numerical investigations of casting processes can be performed on both the macroscopic and microscopic level. However, especially for industrial applications, simulations restricted to the macro level are still usual. They allow the global prediction of mold filling, solidification and stress formation. A rough estimation of the microstructure can be made e.g. by means of criterion functions (1). Some numerical techniques on the micro level have been developed to predict the local evolution of microstructure and the formation of microsegregation as a function of the global cooling conditions. Recent reviews of analytical, semi-empirical and numerical methods can be found in (2, 3). The most advanced models take into account various effects such as solid state diffusion, dendrite arm coarsening and undercooling. As demonstrated by Boettinger et al. (4, 5), the on-line use of thermodynamic programs is advisable to enhance the accuracy of thermodynamic data for multi-component alloys. Micro and macro models should ideally be strongly coupled to take into account mutual influences between microstructural evolution and temperature changes. This paper presents such a fully two-way coupled modeling.

2. Method of Simulation

The described simulation on the macro level are performed by means of the in-house package CASTS, a 3D finite element code. Detailed descriptions and application examples can be found in (6-8).

2.1. Micro Model

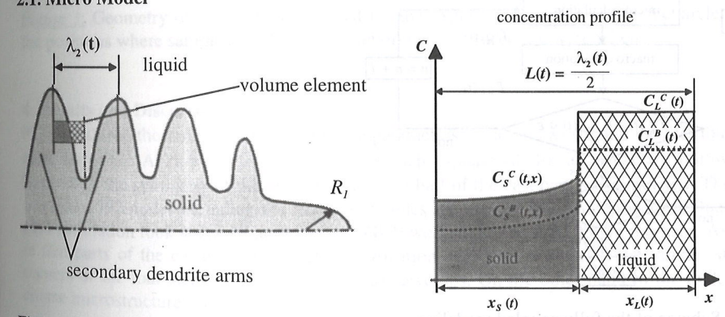

Figure 1: The scheme of the plate model is shown on the left. A qualitative concentration profile of both alloy components *B* and *C* is depicted on the right.

The microsegregation model predicts primary dendrite trunk spacing, λ_1, secondary dendrite arm spacing, λ_2, and phase amounts based on an approach of Roósz and Exner (9) where the complex

dendritic structure is approximated by a plate morphology (see Fig. 1). Although this is just a rough approximation of the dendritic structure, it has been shown that this model yields good agreement between calculation and measurement (9-12). Coarsening is calculated by a semi-empirical equation for the time evolution of λ_2 taken from (9). Complete mixing is assumed in the liquid and the volume element is thought to be at a uniform temperature T. In the solid the concentration profiles of both alloying elements are calculated by solving Fick's second law. All information concerning the phase diagram was calculated with the aid of the programmable thermodynamic calculation interface ChemApp™ (13). It consists of FORTRAN subroutines that allow the calculation of thermodynamic equilibria by minimizing the Gibbs free energy. These subroutines are directly coupled with the simulation program. In the eutectic groove, the growth of primary α-dendrites is assumed to be completed while the secondary α- and β-phases solidify with a Gulliver-Scheil-like behavior. The undercooling of the dendrite tip ΔT^*, consisting of curvature, solutal and gradient undercoolings, is calculated on the basis of the KGT-model. It is considered in the micro model by using the method of Voller and Sundarraj (14). Undercooling of the binary and ternary eutectic has been neglected. The primary spacing is calculated using the approximate equation given in (15). For a detailed description of the numerical procedure see (16).

2.2. Method of Coupling

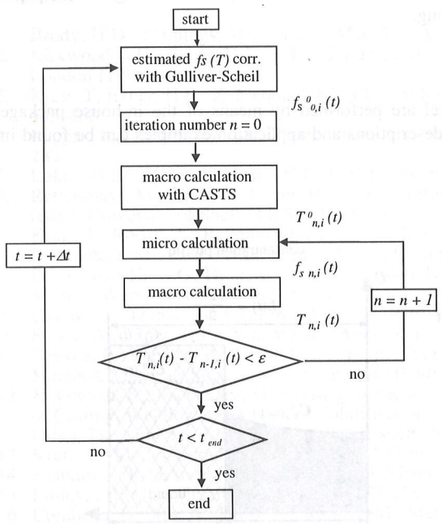

Figure 2: Scheme of the fully coupled modeling

Micro and macro program are linked via the local release of latent heat at each node of the mesh, similar to the method of Sasikumar et al. (17). The scheme of this coupling is illustrated in Fig. 2.

At the beginning of each time step t the iteration loop starts with an estimated fraction solid, f_s, for all nodes i. It determines the release of latent heat from the macro calculation. With this evaluated temperature distribution $T^0_{n,i}(t)$ the micro model simulates the microstructural evolution, leading to a better approximation of f_s which is again input for a repeated macro calculation. This procedure is repeated until sufficient agreement between the temperature distribution of the actual and previous iteration is obtained.

3. Experimental Procedure

In order to validate the described simulation method a step wedge was cast in a permanent mold. Several castings were performed with an AlCu5wt.%Si5wt.%-alloy. The dimensions of the selected casting system are shown in Fig. 3. Due to the different cooling conditions this experimental setup permits the observation of both fine and coarse microstructures. Thermocouples were installed at ten positions to monitor the solidification event. The pouring temperature was 700 °C.

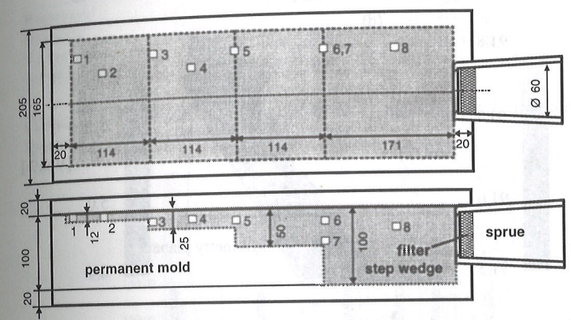

Figure 3: Geometry of the step wedge used for the experimental studies. The rectangles represent the positions where samples for the evaluation of the microstructure were taken.

4. Results and Discussion

Figure 4 shows the calculated microstructure parameters λ_1 (a) and λ_2 (b) and the distribution of the amounts of the Al-rich α-phase (c) and the Si-rich β-phase (d) for an AlCu5wt.%Si5wt.% alloy. Because of the symmetry of the problem, only one half of the cast part was simulated. The FEM-net contains 1392 nodes including the mold. 400 nodes are needed for the step wedge. One fully coupled simulation took about 48 hours on an SGI™ workstation with R10000 processor. As expected, in that parts of the casting where high solidification velocities occur (i.e. the thinner steps or the corners of the four steps) a fine microstructure develops. On the other hand in the bulk material a coarse microstructure occurs.

Due to the very small variation of the phase amounts within the sample the validation of the simulated phase distribution turned out to be very difficult. In the following the comparison between simulation and measurement is thus restricted to the dendrite arm and trunk spacing as it is shown in Figure 5 and 6. The experimental values (black bar in Fig. 5 and 6) are compared with the results of three different simulations. First an uncoupled simulation (dark grey bar) which neglects any mutual

dependency between micro and macro calculation. In addition coupled simulations were performed, with (white bar) and without (light grey bar) consideration of dendrite tip undercooling.

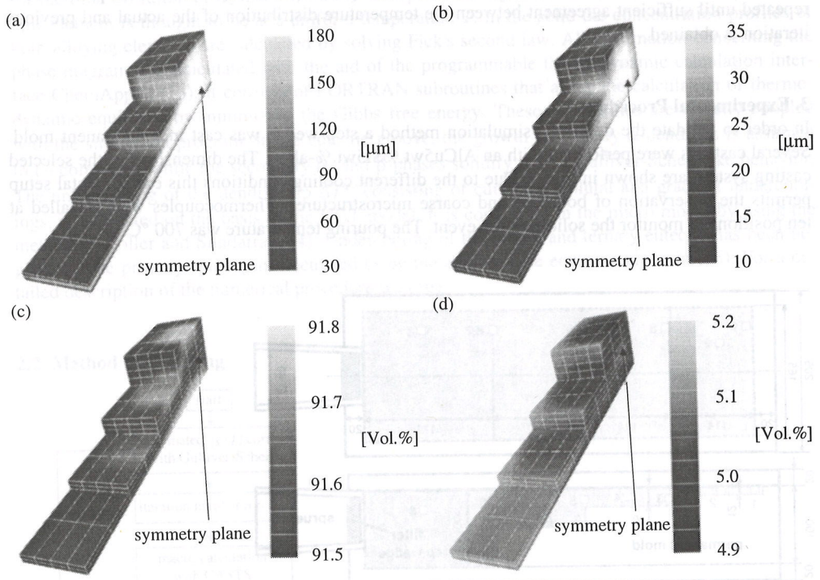

Figure 4: Simulated distributions of the dendrite trunk spacing (a), dendrite arm spacing (b) and the amounts of the Al-rich α-phase (c) and the Si-rich β-phase (d).

It is obvious that there is a good agreement between calculation and measurement for λ_2 especially at positions where a fine microstructure occurs. The deviation between the simulation and experiment for the large values of λ_2 is caused by two different reasons. First, measurements especially on coarse microstructures reveal an unavoidable scatter. Second the material properties especially the diffusion coefficient in the considered ternary alloy are not known precisely. Keeping in mind that the uncoupled calculation takes about half of the time of the fully coupled calculation it must be stated that for this alloy system a complete coupling does not improve the accuracy of the microsimulation remarkably. Further it is obvious that the consideration of dendrite tip undercooling, as described above, increases the deviation between simulation and measurement. This deviation might be caused in an overestimation of the undercooling by the used V-ΔT-relation which is actually only valid for dilute binary alloys.

The reasons for the disagreement in the dendrite trunk spacing λ_1 between simulation and measurement may be caused by the expression used for the calculation of λ_1. It considers a simplified ge-

ometry of the dendritic morphology for directional solidification in binary alloys. However, in the present casting of a ternary alloy only partial columnar growth occurs. Furthermore, the used expression is valid only for steady state solidification. Thus the simulated dendrite trunk spacing can only be interpreted as a rough estimation of order of magnitude.

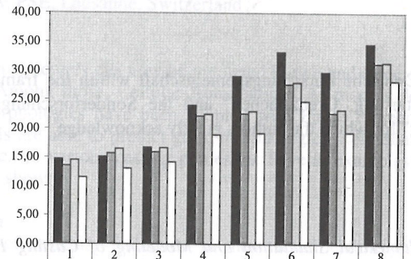

	1	2	3	4	5	6	7	8
experimental	14,70	15,10	16,80	24,07	29,10	33,30	29,80	34,70
uncoupled	13,55	15,70	15,97	22,23	22,63	27,68	22,77	31,31
coupled (no undercooling)	14,53	16,50	16,70	22,55	23,04	27,99	23,34	31,51
coupled (undercooling)	11,54	13,10	14,26	18,98	19,28	24,78	19,41	28,34

Figure 5: Comparison of the experimentally measured and simulated values of the dendrite arm spacing, λ_2. All quantities are given in µm.

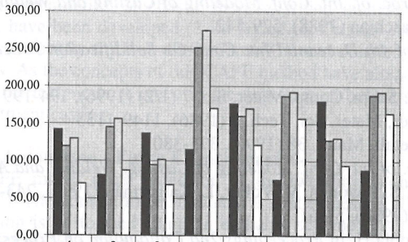

	1	2	3	4	5	6	7	8
experimental	142,00	81,50	136,80	115,40	176,50	75,30	180,30	88,60
uncoupled	119,77	145,32	94,99	251,20	160,48	186,71	128,14	188,13
coupled (no undercooling)	129,83	156,40	101,89	274,63	170,08	192,26	130,80	192,55
coupled (undercooling)	69,85	87,53	68,60	170,57	121,80	157,14	94,47	164,37

Figure 6: Comparison of the experimentally measured and simulated values of the dendrite trunk spacing, λ_1. All quantities are given in µm.

5. Conclusion

A full coupling of a 3D-macro model with a micro model was used to simulate the microstructural evolution during solidification. A thermodynamic calculation interface was used to calculate the

phase diagram information. The results show good agreement with the experiment for the dendrite arm spacing λ_2. The expression used for the calculation of λ_1 turned out to be unsuitable for describing the experiments. For the present alloy system and experimental setup, a complete coupling of the macro and micro model does not enhance the accuracy of the simulation significantly.

Acknowledgement
This work was supported by the Deutsche Forschungsgemeinschaft within the framework of the Graduiertenkolleg "Schmelze, Erstarrung, Grenzflächen" and the Sonderforschungsbereich 370 "Integrative Werkstoffmodellierung" for which the authors greatly acknowledge.

References

(1) P.R. Sahm, P.N. Hansen, *Numerical Simulation and Modeling of Casting Processes for Foundry and Cast-House* (Zürich, Int. Committee of Technical Foundry Association CIATF 1984)
(2) M. Rappaz, Int. Mater. Rev. 34 (1989), 93-123
(3) T. Kraft, H.E. Exner, Z. Metallkd. 87 No. 8 (1996), 598-611 and 652-660
(4) W.J. Boettinger et al., in *Proc. of Int. Conf. Modeling of Casting, Welding and Advanced Solidification Processes VII*, ed. M. Cross, J. Campbell (1995), 649-656
(5) H.E. Exner, M. Rettenmayr, A. Roosz, Mat. Sci. Forum 77 (1991), 205-210
(6) P.N. Hansen, P.R. Sahm, in *Proc. of. Int. Conf. Modeling of Casting and Welding Processes IV*, ed. A.F. Giamei , G.J. Abbaschian (1988), 529-542
(7) M. Fackeldey et al., in *Proc. of 4th Decennial Int. Conf. On Solidification Processing*, Sheffield (1997), 41-44
(8) M. Fackeldey, A. Ludwig, P.R. Sahm, Comp. Mater. Sci. 7 (1/2) (1996), 194-199
(9) A. Roósz, E. Halder, H.E. Exner, Mater. Sci. Tech. 2 (1986), 1149-1155
(10) A. Roósz, H.E. Exner, Acta Metall. Mater. 38 (1990), 375-380
(11) A. Roósz, H.E. Exner, in *Proc. of Int. Conf. Modeling of Casting, Welding and Advanced Solidification Processes VI*, ed. T.S. Piwonka, V. Voller, L. Katgerman (1993), 243-250
(12) T. Kraft, Int. J. Cast Metals, 9 (1996), 51-61
(13) Eriksson G., Spencer P.J., Sippola H, in *Proceedings 2nd Colloquium on Process Simulation*, Helsinki University of Technology, Report TKK-V-B104 (1995) 113
(14) V.R. Voller, S. Sundarraj in *Proc. of Int. Conf. Modeling of Casting, Welding and Advanced Solidification Processes VI*, ed. T.S. Piwonka, V. Voller, L. Katgerman (1993), 251-258
(15) W. Kurz, D.J. Fisher, *Fundamental of Solidification*, 3th edition (Switzerland, Trans Tech Publ. 1992)
(16) K. Greven, M. Fackeldey, A. Ludwig, T. Kraft, M. Rettenmayr, P. R. Sahm, in *Proc. of Int. Conf. Modeling of Casting, Welding and Advanced Solidification Processes VIII*, ed. B.G. Thomas, C. Beckermann (1998), 187-194
(17) R. Sasikumar, H.E Exner, Modeling Simul. Mater. Sci. Eng 1 (1992), 19-27